HHS Public Access

Author manuscript

Gastrointest Endosc. Author manuscript; available in PMC 2022 December 01.

Published in final edited form as:

Gastrointest Endosc. 2021 December ; 94(6): 1119–1130.e4. doi:10.1016/j.gie.2021.06.016.

Endoscopic-mediated, biliary hydrodynamic injection mediating clinically relevant levels of gene delivery in pig liver

Robert L. Kruse[*,1], **Yuting Huang**[*,2,3], **Thomas Shum**[4], **Lu Bai**[5], **Hui Ding**[2,6], **Zack Z. Wang**[7], **Florin M. Selaru**[2,†], **Vivek Kumbhari**[2,8,†]

[1]Department of Pathology, The Johns Hopkins University School of Medicine, Baltimore, MD

[2]Division of Gastroenterology & Hepatology, Department of Medicine, The Johns Hopkins University School of Medicine, Baltimore, MD

[3]Department of Medicine, University of Maryland Medical Center Midtown Campus, Baltimore, MD

[4]Department of Radiology, Brigham and Women's Hospital, Boston, MA

[5]Department of Biology, Johns Hopkins University, Baltimore, MD

[6]Division of Gastroenterology and Hepatology, Renji Hospital, Shanghai Jiao Tong University, Shanghai, China

[7]Division of Hematology, Department of Medicine, The Johns Hopkins University School of Medicine, Baltimore, MD

[8]Division of Gastroenterology & Hepatology, Department of Medicine, Mayo Clinic Florida, Jacksonville, FL

Abstract

Background and Aims: Gene therapy could provide curative therapies to many inherited monogenic liver diseases. Clinical trials have largely focused on adeno-associated viruses (AAV) for liver gene delivery. These vectors, however, are limited by small packaging size, capsid immune responses, and inability to re-dose. As an alternative, nonviral, hydrodynamic injection through vascular routes can successfully deliver plasmid DNA (pDNA) into mouse liver but has achieved limited success in large animal models.

Methods: We explored hydrodynamic delivery of pDNA through the biliary system into the liver of pigs using ERCP, and a power injector to supply hydrodynamic force. Human Factor IX (hFIX), deficient in Hemophilia B, was used as a model gene therapy.

[†]**Corresponding author:** Vivek Kumbhari, vkumbha1@jh.edu; Florin Selaru, fselaru1@jh.edu.
[*]These authors contributed equally

Author contributions: R.L.K, Y.H., V.K, and F.M.S designed experiments. R.L.K, Y.H., T.S., L.B., Z.Z.W. performed experiments. V.K. performed the endoscopic procedure with H.D. assisting. R.L.K, Y.H., V.K., and F.M.S. wrote and revised manuscript.

Competing interests: R.L.K, Y.H., V.K., and F.M.S. have a patent application filed on the work. All other authors do not declare any competing interests.

Results: Biliary hydrodynamic injection was well tolerated without significant changes in vital signs, liver enzymes, hematology, or histology. No off-target pDNA delivery to other organs was detected by PCR. Immunohistochemistry revealed that 50.19% of the liver stained positive for hFIX after hydrodynamic injection at 5.5 mg pDNA, with every hepatic lobule in all liver lobes demonstrating hFIX-expression. hFIX-positive hepatocytes were concentrated around the central vein, radiating outward across all 3 metabolic zones. Biliary hydrodynamic injection in pigs resulted in significantly higher transfection efficiency than mouse vascular hydrodynamic injection at matched pDNA per liver weight dose (32.7-51.9% vs 18.9%, $p<0.0001$).

Conclusions: Biliary hydrodynamic injection via ERCP can achieve higher transfection efficiency into hepatocytes compared with AAV at magnitudes less cost in a clinically relevant human-sized large animal. This technology may serve as a platform for gene therapy of human liver diseases.

Keywords

Gene therapy; hydrodynamic; Non-viral; ERCP; hemophilia

Introduction:

Gene therapy is a long-sought goal for many hereditary liver monogenic diseases, including hemophilia, Wilson's Disease, alpha-1 antitrypsin disease, and phenylketonuria. The most promising gene delivery system, so far, has been adeno-associated virus (AAV) vectors, which have achieved some success in clinical trials. AAV is a nonenveloped virus with 4.8 kb genome, and can mediate efficient liver transduction in mouse and primate models.[1]

However, several challenges with AAV vectors have occurred as they have advanced into humans. In early clinical studies for hemophilia B, the highest AAV dose yielded 12% of normal hFIX levels, but a T-cell response against AAV capsid protein developed and transgene expression was lost.[2] Steroids were used in later studies to inhibit T-cell responses.[3,4] Other concerns include the gradual decline in expression over time due to the episomal status of the genome, which is particularly challenging in pediatric patients with growing livers,[5] but also seen in an adult hemophilia A trial with a progressive decline in Factor VIII activity over 3 years.[6] Redosing AAV gene therapy could alleviate the loss of genome, but the development of antibodies against the AAV capsid after the first administration precludes it.[7] Even before first dosing, 30% to 70% of the population has antibodies against common AAV serotypes, making them ineligible for treatment.[8]

As an alternative, a nonviral, redosable gene delivery strategy could be transformative. Hydrodynamic tail vein injection (HTVI) of naked DNA has been a convenient method to deliver genes into mouse livers,[9] can be redosed multiple times,[9] and can achieve therapeutic hFIX levels in mice for 1.5 years after injection.[10] HTVI causes temporary right heart failure and hepatic congestion in mice, creating pores in the hepatocyte membrane for DNA delivery inside cells.[11] Importantly, hydrodynamic delivery does not pose any size constraints on the DNA vector (>100 kb achieved), unlike AAV. [12] Translating hydrodynamic gene delivery into the liver of large animals has proven to be a formidable challenge, however, requiring catheterization procedures to isolate liver venous systems to

deliver local hydrodynamic pressure.[13,14] A liver lobe-specific vascular injection procedure in pigs can achieve gene expression,[15] but the overall expression levels in large animals remain significantly lower than in mice.[16] A pilot clinical trial of vascular hydrodynamic injection into the liver of human patients to express thrombopoietin was well-tolerated, but did not achieve increases in platelet counts.[17]

An alternative strategy for liver-directed hydrodynamic delivery is to inject DNA through the biliary tract.[18,19] The biliary tract contacts all hepatocytes through a parallel, counterflow network to hepatic sinusoids within liver lobules,[20] eventually draining bile through the common hepatic duct (CHD) and into the small intestine. The total volume of the biliary tract (~30 mL)[21] is significantly lower than the total liver blood volume (~600 mL).[22] The biliary system is routinely accessed clinically via ERCP, of which 350 to 500,000 procedures are performed in the United States annually.[23] We previously investigated biliary hydrodynamic delivery, achieving proof-of-concept that DNA could be delivered into all lobes and mediate stable protein expression.[24] However, hepatocyte transfection efficiency, localization and distribution of transfected hepatocytes, key safety data including off-target transfection are required before human use.

Herein, we sought to increase the efficiency of biliary hydrodynamic injection to levels suitable to treat human disease, as well as to quantify the transfection efficiency. Given the potential risks of hydrodynamic injection, we also investigated multiple different safety aspects of the procedure. We chose to use pigs as our model, which have similar organ size to human patients, and used commercially available equipment used currently in clinical care to ensure all DNA dosing and procedures would be clinically translatable for human patients,

Methods:

Animal experiments

All animal experiments were conducted under the approval of the animal care and use committee of Johns Hopkins University and adhere to the guidelines of the NIH Guide for the Care and Use of Laboratory Animals. Mouse experiments were performed on C57BL/6 strain (Jackson Labs). Yorkshire pigs were acquired from Archer Farms, Darlington, MD. All pigs were female and were acquired for their targeted weight before procedure. Pigs were acclimated and housed in conditions as previous described.[24]

Endoscopy Procedure

Food was withheld from pigs the night before the procedure, and all pigs were weighed before the procedure for proper anesthetic doses. Once sedated, pretreatment blood draws and stool were collected. Vital signs were monitored throughout the procedure by a veterinary technician. An endoscope (therapeutic video duodenoscope, ED-580XT, FUJIFILM Medical Systems U.S.A.) was advanced into the small intestine. A sphincterotome (CleverCut 3V, Olympus Medical) preloaded with a 0.025-inch hydrophilic guidewire (VisiGlide, Olympus Medical) was then advanced into the common hepatic duct (CHD) as verified by fluoroscopy using 4 to 5 mL of radiocontrast solution (Omnipaque,

350 mg/mL; GE Health Co) and a Philips Allura C-Arm. The sphincterotome was then exchanged over the wire for an extraction balloon catheter (Multi-SV Plus, Olympus Medical) with the balloon catheter being inflated to 11.5 mm at the CHD 1 to 2 cm below the hepatic hilum. A power injector (MEDRAD Mark 7 Arterion, Bayer) was filled with plasmid DNA (pDNA) solution and attached to the catheter injection port. Injection parameters were executed as listed in Supplementary Table 1. The balloon was deflated 5 seconds after injection, and repeat fluoroscopy with 4 to 5 mL of contrast injection was performed to assess the intact biliary system. Transabdominal ultrasound was performed on pig no. 2 by a board-certified radiologist before and after hydrodynamic injection. Post-treatment blood draw and post-treatment stool were then obtained. Total procedure time was monitored from insertion of the endoscope through injection and removal of the endoscope. Specific details on anesthesia doses for the procedure are provided in the enclosed reference.[24]

Additional methods can be found in Appendix 1.

Results:

Biliary hydrodynamic injection procedure

We chose to use hFIX as a model gene to deliver into pigs, given its extensive investigation in different gene therapy models and in clinical trials. As a first step, we aimed to deliver an hFIX DNA expression cassette currently used in AAV clinical trials,[3,4,25] ensuring high-level expression, and combined it with hyperactive piggyBac (hyPBase) transposase for gene integration. The latter has increased expression in mouse models and serves to avoid gene silencing of the injected plasmid DNA. We validated the gene vectors in mice, yielding efficient hFIX expression after HTVI more than 200% over normal human levels (Supplementary Figure 1). For biliary hydrodynamic injection, we used parameters of 30 mL of volume injected at a flow rate of 2 mL/sec (Supplementary Table 1).[24] Two doses of hFIX DNA transposon were used, 3 mg and 5.5 mg, at similar transposon to transposase ratios, to evaluate whether any dose dependence in hFIX expression was observed (Supplementary Table 1).

For our studies, 4 female Yorkshire pigs weighing between 35 to 37 kilograms were obtained. During each procedure, an endoscope was advanced into the small intestine and the ampulla of Vater was visualized (Figure 1A). An occlusion balloon tipped catheter was advanced through the working channel of the endoscope, through the ampulla, and into the common bile duct and eventually the common hepatic duct (CHD). Before pDNA injection, retrograde contrast injection opacified the biliary tree to ensure the catheter placement would result in access to the entire liver parenchyma and that no aberrant ductal anatomy was present (Figure 1B and C). Biliary hydrodynamic injection itself is able to deliver contrast solution into all lobes of the liver in a separate pig experiment, whereas after hydrodynamic injection, repeat fluoroscopy demonstrated that the biliary system remains intact without leakage of contrast solution into the liver parenchyma or abdominal cavity (Figure 1D and E). The 4 ERCP hydrodynamic procedures averaged 43 ± 11 minutes.

Safety of biliary hydrodynamic injection

We next evaluated the potential for injury from biliary hydrodynamic injection. The gallbladder measured with transabdominal ultrasound pre- and postprocedure did not demonstrate changes in size, confirming balloon seal prevented fluid entry into this space (Supplementary Figure 2A). Vital signs taken did not show any acute changes in blood pressure, heart rate, pulse oximetry, or respiratory tidal volumes from pre- to postprocedure (Figure 1E; Supplementary Figure 2B).

In the time after hydrodynamic injection, there were no significant changes in liver transaminases, total or direct bilirubin, albumin, and gamma-glutamyl transferase (Figure 1F). No leukocytosis in the 4 days afterinjection was observed, whereas hemoglobin, red blood cell count, platelet values did not show significant changes (Figure 1G). Pigs displayed normal growth patterns (~1 kg per week) posthydrodynamic injection, increasing weight from 35.33 ± 0.33 kg to 38.83 ± 0.33 kg in 3 weeks ($p=0.0018$).

We selected pig no. 3 for tissue analysis at 1 week after injection because it received a higher pDNA dose. Moreover, this timepoint is before any potential immune response against hFIX. Upon necropsy of pig no. 3, gross visual inspection of the visceral and diaphragmatic surfaces of the liver exhibited no abnormalities (Figure 2A and B). The biliary tract including the right and left hepatic bile ducts was intact during dissection (Figure 2C), confirming post-injection fluoroscopic imaging (Figure 1D). Liver histology resembled an uninjected pig, with no immune infiltrate or necrosis (Figure 2D).

Bile collected at 1 week after injection was negative for hFIX DNA, confirming degradation by that time point (Figure 2E). Because pDNA in the bile ducts eventually drains into the small intestine, we evaluated if any pDNA is taken up by pig intestinal bacteria. Stool DNA collected from 2 pigs was negative for hFIX DNA at all time points (Figure 2F).

Off-target gene delivery into other tissues beyond the liver was next evaluated. PCR testing revealed the presence of pDNA in the plasma 15 minutes after injection (Figure 2E), explained by the escape of fluid from biliary canaliculi through hepatocyte tight junctions and into liver venous circulation.[19] By day 1 after injection, pDNA was absent, consistent with degradation by serum DNases.[26,27] Different tissues (23 in total) were also investigated for transfection. All tissues were negative for hFIX DNA by PCR indicating no pDNA delivery (Figure 2G).

Evaluation of human FIX gene expression in pigs

Samples were taken in proximal and distal portions of every liver lobe in relation to the hydrodynamical injection point in the CHD given potential variation in hydrodynamic pressure (Figure 3A). We observed delivery of the hFIX DNA into all pig liver lobes at one week (Figure 3B) and 3 weeks (Supplementary Figure 3) after hydrodynamic injection. RNA expression was observed in every liver lobe, indicating pDNA presence inside the nucleus (Figure 3C). hFIX protein was next evaluated by western blot. Examining antibody specificity, the hFIX antibody stained the correct hFIX protein size (70 kDa) in human plasma, whereas a low level of porcine FIX cross-reactivity was observed in pig plasma, calculated to be 6.4% (Supplementary Figure 4).

Western blot of pig liver tissue demonstrated clear bands of hFIX staining in all hFIX gene injected liver lobes at varying expression levels (Figure 3D), with only low-level cross-reactivity detected in un-injected pig liver. Semi-quantitative analysis of normalized band intensity demonstrated all hFIX-injected bands were well above uninjected control liver (Figure 3D). Tissue hFIX protein level was calculated to be 10.11% ± 4.05% of the control pig liver's porcine factor IX level. Plasma levels of hFIX in all 4 pigs were negative at day 1 and day 4 after injection, as expected, consistent with a lack of hFIX secretion seen in hFIX-transgenic pigs.[28]

Analysis of transfection efficiency of hFIX in pig liver

Hepatocytes positive for hFIX were observed by immunohistochemistry (IHC) in the injected pig liver. The hFIX stain was cytoplasmic within hepatocytes of injected pigs, matching hFIX staining in a human liver control (Figure 4A). Across entire tissue sections, we observed hFIX-positive hepatocytes around 100% of central veins analyzed and within every lobule (Figure 4B). Although the most intense immunostaining was observed around the central vein, hFIX-positive hepatocytes could be identified across all 3 metabolic zones, including near the portal triad (Supplementary Figure 5).

hFIX-positive hepatocytes were present in all 4 pigs injected and in every liver lobe tested (Figure 5A), indicating that a single CHD injection site could reach all liver lobes efficiently. We quantified the transfection efficiency by calculating the hFIX stained area within multiple lobules per section. There was no clear right versus left liver predominance in transfection efficiency (Figure 5A), whereas proximal and distal tissue sections to the CHD injection site had generally similar hFIX-positive area percentage (Figure 5B). There was a trend toward a dose dependent response to plasmid DNA, with a significant difference in the percentages of hFIX-positive cells from pig no. 1 (3 mg) and the two 5.5 mg dosed pigs (pig no. 3, no. 4) (Figure 5C).

Comparing mouse HTVI and biliary hydrodynamic injection

We next sought to analyze mouse HTVI versus pig biliary hydrodynamic injection in terms of percent hepatocyte transfection. Biliary hydrodynamic injection in pigs unexpectedly yielded significantly more hFIX-positive hepatocytes than an HTVI method in mice (Figure 6A and C).

Mouse HTVI yielded hFIX-positive hepatocytes primarily in proximity to the central vein, although often not directly adjacent to the central vein, and almost never in periportal areas of the lobule (Figure 6A). By comparison, pig hydrodynamic injection was also strongest around the central vein, with almost uniform transfection of cells adjacent to the central vein; hFIX-positive periportal hepatocytes could be readily detected as well. Concerning the localization of hepatocytes, the different distributions within zones of the hepatic lobule between species are likely explained by the different routes/mechanisms of injection (Figure 6B). Both techniques were efficient at delivery to every lobule (Figure 4B, Supplementary 6).

Discussion:

In this study, we have investigated the ability to translate hydrodynamic gene delivery into a large animal model. To improve on vascular strategies, we hypothesized that the biliary system offers a safer and technically simpler route for hydrodynamic injection. We found that pigs tolerated the procedure with no acute changes in vital signs. Moreover, unlike AAV gene therapy where the vector transduces many off-target issues,[1] we were only able to find pDNA inside the liver. Overall, we found hFIX expression in every lobule of every lobe in every pig that underwent the procedure, with no clear transfection preference between the right and left liver lobes. Hepatocytes in the periportal and pericentral regions of the lobule were transfected. All pigs continued expressing hFIX until the end of the experiment at 3 weeks, suggesting expression stability and immune tolerance, given that adaptive immune responses typically form by 2 weeks. Of note, a similar hyPBase transposon experiment in mice showed stable hFIX expression for 1 year.[29] Although there is reason to hypothesize that the expression in pigs could be observed at similarly long time points, a future study is needed to obtain experimental proof.

Impressively, we found 50.19% ± 3.50% of hepatocytes were hFIX-positive in the high-dose pDNA pigs. The majority of transfected cells clustered around the central vein, radiating outward along the hepatic sinusoids. hFIX-positive hepatocytes, usually with weaker expression, could also be observed in periportal areas along lobular borders. Comparing our non-viral liver transfection efficiency in pigs to AAV vector transduction efficiency in large animal studies, we observed higher transfection efficiency in our study (32.7%-51.9%) compared with ssAAV8, which yielded an average 17% transduced area in cynomolgus and rhesus macaques at 3×10^{12} GC/kg dose,[30] and to scAAV3B, which yielded 36% in rhesus macaques at a dose of 1×10^{13} GC/kg.[31] Importantly, we observed significant hFIX protein expression (10.11% ± 4.05% of pig FIX level) in liver tissue, which could portend clinically significant hFIX plasma levels in a different animal model that secretes hFIX efficiently. Future increases in pDNA dose and/or injection parameters[32] may yield additional gains to increase hepatocyte transfection, which is suggested by the increased transfection area at the higher 5.5 mg DNA dose.

The high transfection efficiency achieved in our study greatly exceeds that which intracellular protein liver disorders such as Wilson's Disease (20%)[33] and Crigler-Najjar (1-2%)[34] require for clinical cure, suggesting significant promise for the biliary hydrodynamic approach. Future studies will evaluate biliary hydrodynamic gene delivery of hFIX in animal models such as dogs and non-human primates to gauge plasma hFIX plasma levels, given the inability of pigs to secrete hFIX. Indeed, a transgenic pig with hFIX cDNA inserted into the pig FIX locus under the endogenous promoter yielded strikingly low hFIX plasma levels (~80 ng/mL vs 5000 ng/mL in humans),[28] supporting that pigs have a fundamental biological difference that prevents their hepatocytes from efficiently secreting hFIX.

Compared with prior vascular hydrodynamic approaches in pigs, our biliary hydrodynamic injection requires significantly less volume of fluid (30 mL total liver vs 200-300 mL per lobe), slower flow rates (2 mL/sec vs 20-100 mL/sec), and smaller DNA doses (3-5

mg for the whole liver vs 15-20 mg per liver or liver lobe) for gene delivery.[14,35–37] Despite these higher parameters and DNA doses, vascular approaches demonstrated at best achieved only 5% to 15% transfection efficiency in individual liver lobes.[14,35–37] Vascular hydrodynamic injection in pigs also generally elicited higher ALT/AST spikes (100-200 U/L) after injection compared with no elevation in the current study.[35] In comparison with our previous study of biliary injection, the order of magnitude improvements in transfection efficiency likely relates to the use of powerful liver-specific promoters, as well as a more efficient transposition, exemplified by a lower ratio of transposon: transposase plasmid injected (7:1 vs 25:1), and a more hyperactive transposon activity. All of these elements greatly improved expression from HTVI in a mouse model.[29]

Concerning the limitations of biliary hydrodynamic injection, there is the potential for pancreatitis with ERCP procedure in human patients, although, given the injection location in CHD close to the liver, there should be no higher risk than with a typical, clinical grade ERCP procedure. We were unable to model this potential risk in pigs, as they have separate ducts for bile and pancreas and do not develop post-ERCP pancreatitis. However, due to the inherent risk for post-ERCP pancreatitis, many different strategies have recently been developed to decrease this risk.[38] Last, the relative morbidity of many of the monogenic diseases to be treated with this technology likely outweighs this risk of procedure. Another limitation is that pig liver lobules also have more fibrous tissue surrounding them versus humans, which may also modulate the procedure.[15] A third limitation could be for certain indications, liver fibrosis could potentially lower hydrodynamic transfection efficiency by obstructing fluid flow.[39]

In conclusion, we demonstrate that hydrodynamic gene delivery into the liver through the biliary tract in pigs has higher levels of transfection efficiency than AAV-mediated vectors, while possessing no toxicity. Important for clinical translation, pDNA production costs for biliary hydrodynamic approach are 200-fold lower when compared with AAV vector production. Furthermore, the successful use of medical devices used in clinical practice for this gene delivery procedure suggests the potential for rapid clinical translation using the same parameters described in this study. Future investigations will continue to optimize DNA doses and injection settings for individual monogenic diseases in preparation for pilot clinical trials.

Supplementary Material

Refer to Web version on PubMed Central for supplementary material.

Acknowledgements:

We thank the assistance of Rebecca Krimins, Virginia Bogdan, Juls Meyer, Mohamad Itani, Yervant Ichkhanian, and Cem Simsek during pig experiments; Katelynn Davis with pig necropsy; Kevan Salimian and Johnson Wang on IHC interpretation; Haiqing Zhao with western blot.

Funding:

This study was supported by the Johns Hopkins Hospital GI Core Center Pilot Project grant (1P30DK089502-01).

Glossary

AAV	adeno-associated viruses
ALT	alanine aminotransferase
AST	aspartate animotransferase
CHD	common hepatic duct
CMV	cytomegalovirus
CTL	control
DNA	deoxyribonucleic acid
ERCP	endoscopic retrograde cholangiopancreatography
GC	genome copy
GGT	gamma-glutamyl transferase
H&E	hematoxylin and eosin
hAAT	human alpha-1 antitrypsin
hFIX	human factor IX
hyPBase	hyper active piggyBac transposase
HTVI	hydrodynamic tail vein injection
IHC	immunohistochemistry
LML	left medial lobe
LLL	left lateral lobe
PCR	polymerase chain reaction
pDNA	plasmid DNA
PLT	platelet
Q	quadrate
RBC	red blood cell
RML	right medial lobe
RNA	ribonucleic acid
RLL	right lateral lobe
SEM	standard error of mean
TR	terminal repeats

UTR	untranslated region
WBC	white blood cell

References

1. Wang D, Tai PWL, Gao G. Adeno-associated virus vector as a platform for gene therapy delivery. Nat Rev Drug Discov. Nature Publishing Group; 2019;18:358–78. [PubMed: 30710128]
2. Manno CS, Pierce GF, Arruda VR, Glader B, Ragni M, Rasko JJ, et al. Successful transduction of liver in hemophilia by AAV-Factor IX and limitations imposed by the host immune response. Nature Medicine. Nature Publishing Group; 2006;12:342–7.
3. Nathwani AC, Tuddenham EGD, Rangarajan S, Rosales C, McIntosh J, Linch DC, et al. Adenovirus-associated virus vector-mediated gene transfer in hemophilia B. N Engl J Med. 2011;365:2357–65. [PubMed: 22149959]
4. Nathwani AC, Reiss UM, Tuddenham EGD, Rosales C, Chowdary P, McIntosh J, et al. Long-term safety and efficacy of factor IX gene therapy in hemophilia B. N Engl J Med. 2014;371:1994–2004. [PubMed: 25409372]
5. Kok CY, Cunningham SC, Carpenter KH, Dane AP, Siew SM, Logan GJ, et al. Adeno-associated virus-mediated rescue of neonatal lethality in argininosuccinate synthetase-deficient mice. Mol Ther. 2013;21:1823–31. [PubMed: 23817206]
6. Pasi KJ, Rangarajan S, Mitchell N, Lester W, Symington E, Madan B, et al. Multiyear Follow-up of AAV5-hFVIII-SQ Gene Therapy for Hemophilia A. N Engl J Med. 2020;382:29–40. [PubMed: 31893514]
7. Manning WC, Zhou S, Bland MP, Escobedo JA, Dwarki V. Transient immunosuppression allows transgene expression following readministration of adeno-associated viral vectors. Human Gene Therapy. 1998;9:477–85. [PubMed: 9525309]
8. Calcedo R, Morizono H, Wang L, McCarter R, He J, Jones D, et al. Adeno-associated virus antibody profiles in newborns, children, and adolescents. Clin Vaccine Immunol. 11 ed. American Society for Microbiology; 2011;18:1586–8. [PubMed: 21775517]
9. Liu F, Song Y, Liu D. Hydrodynamics-based transfection in animals by systemic administration of plasmid DNA. Gene Therapy. Nature Publishing Group; 1999;6:1258–66. [PubMed: 10455434]
10. Miao CH, Thompson AR, Loeb K, Ye X. Long-term and therapeutic-level hepatic gene expression of human factor IX after naked plasmid transfer in vivo. Mol Ther. 2001;3:947–57. [PubMed: 11407909]
11. Zhang G, Gao X, Song YK, Vollmer R, Stolz DB, Gasiorowski JZ, et al. Hydroporation as the mechanism of hydrodynamic delivery. Gene Therapy. 2004;11:675–82. [PubMed: 14724673]
12. Hibbitt OC, Harbottle RP, Waddington SN, Bursill CA, Coutelle C, Channon KM, et al. Delivery and long-term expression of a 135 kb LDLR genomic DNA locus in vivo by hydrodynamic tail vein injection. J Gene Med. John Wiley & Sons, Ltd; 2007;9:488–97. [PubMed: 17471590]
13. Yoshino H, Hashizume K, Kobayashi E. Naked plasmid DNA transfer to the porcine liver using rapid injection with large volume. Gene Therapy. Nature Publishing Group; 2006;13:1696–702. [PubMed: 16871229]
14. Aliño SF, Herrero MJ, Noguera I, Dasí F, Sánchez M. Pig liver gene therapy by noninvasive interventionist catheterism. Gene Therapy. Nature Publishing Group; 2007;14:334–43. [PubMed: 17036058]
15. Kamimura K, Suda T, Xu W, Zhang G, Liu D. Image-guided, Lobe-specific Hydrodynamic Gene Delivery to Swine Liver. Mol Ther. Elsevier; 2009;17:491–9. [PubMed: 19156134]
16. Fabre JW, Grehan A, Whitehorne M, Sawyer GJ, Dong X, Salehi S, et al. Hydrodynamic gene delivery to the pig liver via an isolated segment of the inferior vena cava. Gene Therapy. Nature Publishing Group; 2008;15:452–62. [PubMed: 18004400]
17. Khorsandi SE, Bachellier P, Weber JC, Greget M, Jaeck D, Zacharoulis D, et al. Minimally invasive and selective hydrodynamic gene therapy of liver segments in the pig and human. Cancer Gene Ther. Nature Publishing Group; 2008;15:225–30. [PubMed: 18259214]

18. Zhang G, Vargo D, Budker V, Armstrong N, Knechtle S, Wolff JA. Expression of naked plasmid DNA injected into the afferent and efferent vessels of rodent and dog livers. Human Gene Therapy. 1997;8:1763–72. [PubMed: 9358026]

19. Hu J, Zhang X, Dong X, Collins L, Sawyer GJ, Fabre JW. A remarkable permeability of canalicular tight junctions might facilitate retrograde, non-viral gene delivery to the liver via the bile duct. Gut. BMJ Publishing Group; 2005;54:1473–9. [PubMed: 15985562]

20. Chen Y, Bai L, Zhou Y, Zhang X, Zhang J, Shi Y. Fine-scale visualizing the hierarchical structure of mouse biliary tree with fluorescence microscopy method. Biosci Rep. 2020;40:609.

21. Ludwig J, Ritman EL, LaRusso NF, Sheedy PF, Zumpe G. Anatomy of the human biliary system studied by quantitative computer-aided three-dimensional imaging techniques. Hepatology. John Wiley & Sons, Ltd; 1998;27:893–9. [PubMed: 9537426]

22. Kjekshus H, Risoe C, Scholz T, Smiseth OA. Regulation of hepatic vascular volume: contributions from active and passive mechanisms during catecholamine and sodium nitroprusside infusion. Circulation. 1997;96:4415–23. [PubMed: 9416912]

23. Cappell MS, Friedel DM. Stricter national standards are required for credentialing of endoscopic-retrograde-cholangiopancreatography in the United States. WJG. 2019;25:3468–83. [PubMed: 31367151]

24. Kumbhari V, Li L, Piontek K, Ishida M, Fu R, Khalil B, et al. Successful liver-directed gene delivery by ERCP-guided hydrodynamic injection (with videos). Gastrointest Endosc. 2018;88:755–5. [PubMed: 30220303]

25. Nathwani AC, Gray JT, Ng CYC, Zhou J, Spence Y, Waddington SN, et al. Self-complementary adeno-associated virus vectors containing a novel liver-specific human factor IX expression cassette enable highly efficient transduction of murine and nonhuman primate liver. Blood. 2006;107:2653–61. [PubMed: 16322469]

26. Kawabata K, Takakura Y, Hashida M. The fate of plasmid DNA after intravenous injection in mice: involvement of scavenger receptors in its hepatic uptake. Pharm Res. Kluwer Academic Publishers-Plenum Publishers; 1995;12:825–30. [PubMed: 7667185]

27. Liu F, Shollenberger LM, Conwell CC, Yuan X, Huang L. Mechanism of naked DNA clearance after intravenous injection. J Gene Med. John Wiley & Sons, Ltd; 2007;9:613–9. [PubMed: 17534886]

28. Chen J, An B, Yu B, Peng X, Yuan H, Yang Q, et al. CRISPR/Cas9-mediated knockin of human factor IX into swine factor IX locus effectively alleviates bleeding in hemophilia B pigs. Haematologica. Haematologica; 2020 23;:haematol.2019.224063.

29. Di Matteo M, Samara-Kuko E, Ward NJ, Waddington SN, Waddingon SN, McVey JH, et al. Hyperactive piggyBac transposons for sustained and robust liver-targeted gene therapy. Mol Ther. 2014;22:1614–24. [PubMed: 25034357]

30. Wang L, Calcedo R, Bell P, Lin J, Grant RL, Siegel DL, et al. Impact of pre-existing immunity on gene transfer to nonhuman primate liver with adeno-associated virus 8 vectors. Human Gene Therapy. 2011;22:1389–401. [PubMed: 21476868]

31. Li S, Ling C, Zhong L, Li M, Su Q, He R, et al. Efficient and Targeted Transduction of Nonhuman Primate Liver With Systemically Delivered Optimized AAV3B Vectors. Mol Ther. 2015;23:1867–76. [PubMed: 26403887]

32. Huang Y, Kruse RL, Ding H, Itani MI, Morrison J, Wang ZZ, et al. Parameters of biliary hydrodynamic injection during endoscopic retrograde cholangiopancreatography in pigs for applications in gene delivery. PLoS ONE. Public Library of Science; 2021;16:e0249931. [PubMed: 33909609]

33. Murillo O, Moreno D, Gazquez C, Barberia M, Cenzano I, Navarro I, et al. Liver Expression of a MiniATP7B Gene Results in Long-Term Restoration of Copper Homeostasis in a Wilson Disease Model in Mice. Hepatology. John Wiley & Sons, Ltd; 2019;70:108–26. [PubMed: 30706949]

34. Greig JA, Nordin JML, Draper C, McMenamin D, Chroscinski EA, Bell P, et al. Determining the Minimally Effective Dose of a Clinical Candidate AAV Vector in a Mouse Model of Crigler-Najjar Syndrome. Mol Ther Methods Clin Dev. 2018;10:237–44. [PubMed: 30112420]

35. Kamimura K, Suda T, Zhang G, Aoyagi Y, Liu D. Parameters Affecting Image-guided, Hydrodynamic Gene Delivery to Swine Liver. Mol Ther Nucleic Acids. 2013;2:e128. [PubMed: 24129227]

36. Sendra L, Miguel A, Pùrez-Enguix D, Herrero MJ, Montalvá E, García-Gimeno MA, et al. Studying Closed Hydrodynamic Models of “In Vivo” DNA Perfusion in Pig Liver for Gene Therapy Translation to Humans. Stieger K, editor. PLoS ONE. Public Library of Science; 2016;11:e0163898. [PubMed: 27695064]

37. Sendra L, Herrero MJ, Aliño SF. Translational Advances of Hydrofection by Hydrodynamic Injection. Genes (Basel). Multidisciplinary Digital Publishing Institute; 2018;9:136.

38. Thiruvengadam NR, Kochman ML. Emerging Therapies to Prevent Post-ERCP Pancreatitis. Curr Gastroenterol Rep. Springer US; 2020;22:59–10. [PubMed: 33188441]

39. Kobayashi Y, Kamimura K, Abe H, Yokoo T, Ogawa K, Shinagawa-Kobayashi Y, et al. Effects of Fibrotic Tissue on Liver-targeted Hydrodynamic Gene Delivery. Mol Ther Nucleic Acids. 2016;5:e359. [PubMed: 27574785]

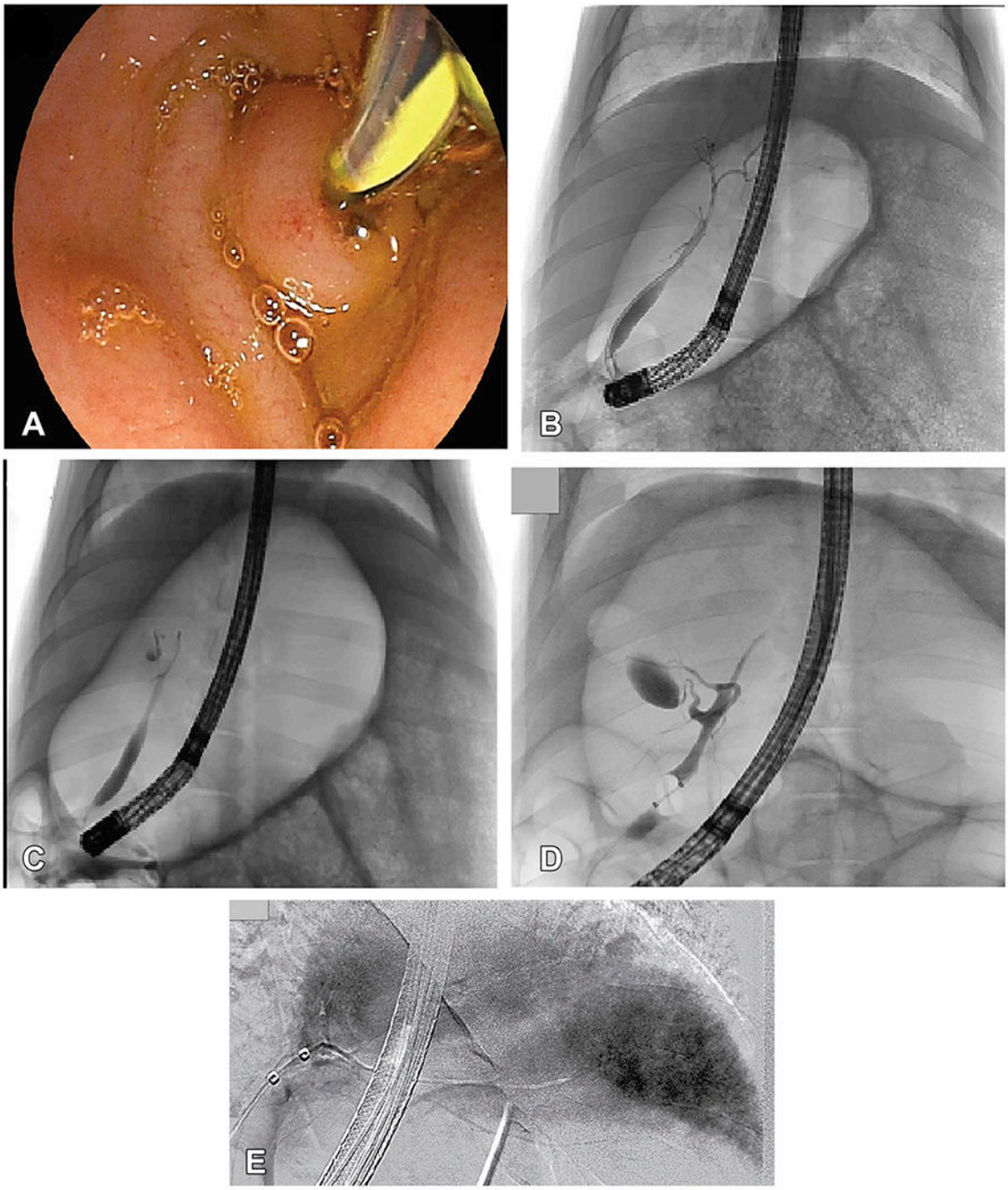

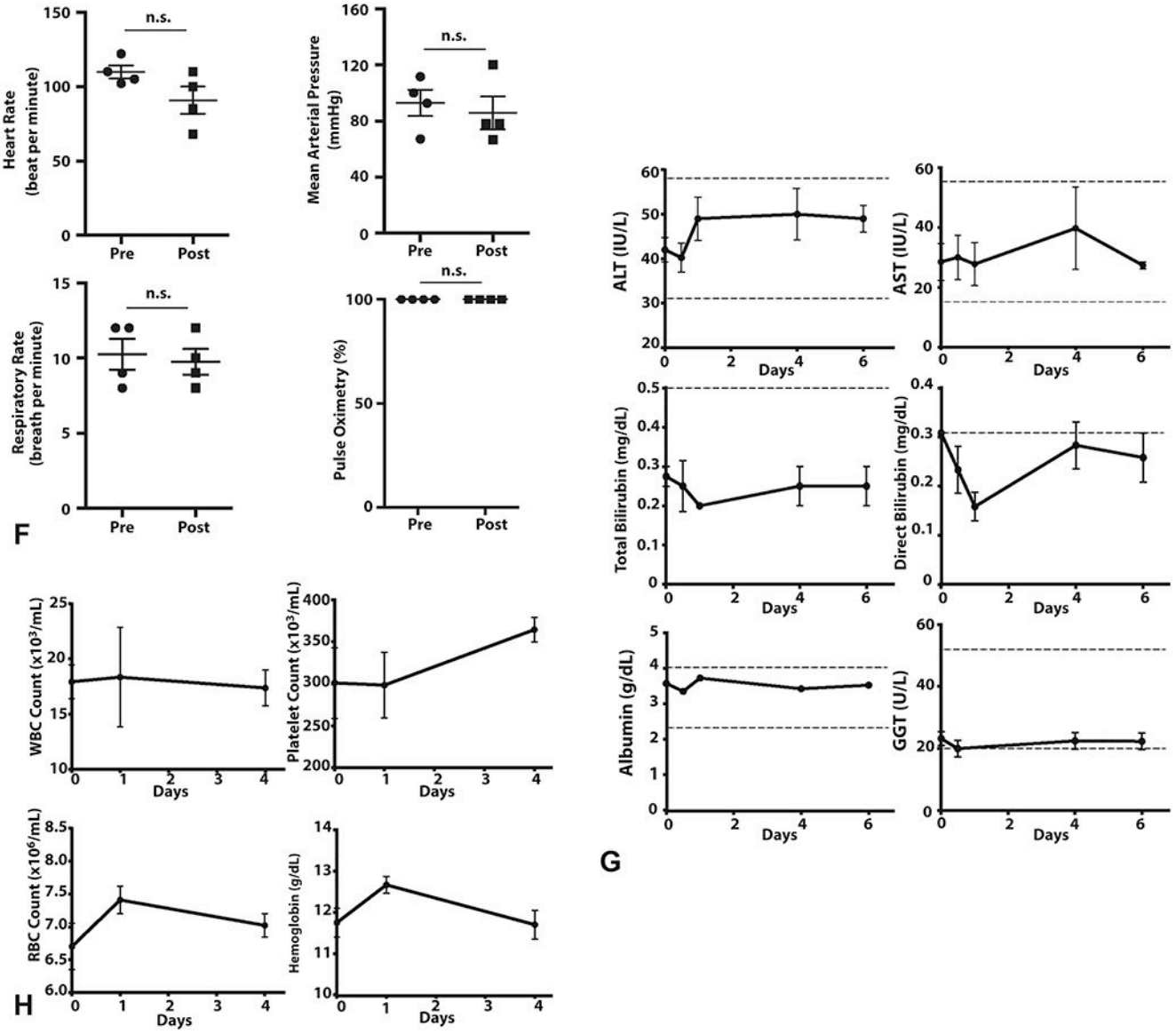

Figure 1. ERCP-mediated hydrodynamic injection is well tolerated by pigs.

A, Cannulation of the ampulla of Vater during endoscopy in pig no. 2 is depicted. B-D, Fluoroscopic imaging with contrast is used during ERCP to visualize the biliary tree. (B) Branches of the biliary tree are displayed before injection in pig no. 1. C and D, Contrast injection with the balloon inflated in the common bile duct after hydrodynamic injection reveals an intact biliary system as evidenced by no contrast extravasation (pig no. 1, C, pig no. 3, D). E, A representative image from a pig in a separate experiment illustrated acinarization of the whole liver during hydrodynamic injection of contrast solution. F, For all 4 pigs, the values of the heart rate the mean arterial pressure, the respiratory rate, and pulse oximetry were compared before and after the procedure, demonstrating no significant difference. An unpaired, parametric, 2-tailed t-test was used for analysis; significance ($P<0.05$). G, Liver function biomarkers (ALT, AST, total/direct bilirubin, albumin, GGT) were monitored after hydrodynamic injection showing no significant

changes. H, Hematologic parameters monitored after hydrodynamic injection show minimal effects. Day 0 = injection day, pre-injection sample. The 15-minute postinjection sample is set at 0.5 days for representative purposes. Alanine Aminotransferase (ALT); Aspartate Aminotransferase (AST); Gamma-glutamyl Transferase (GGT); White blood cell (WBC); Platelet (PLT) ; Red blood cell (RBC) count

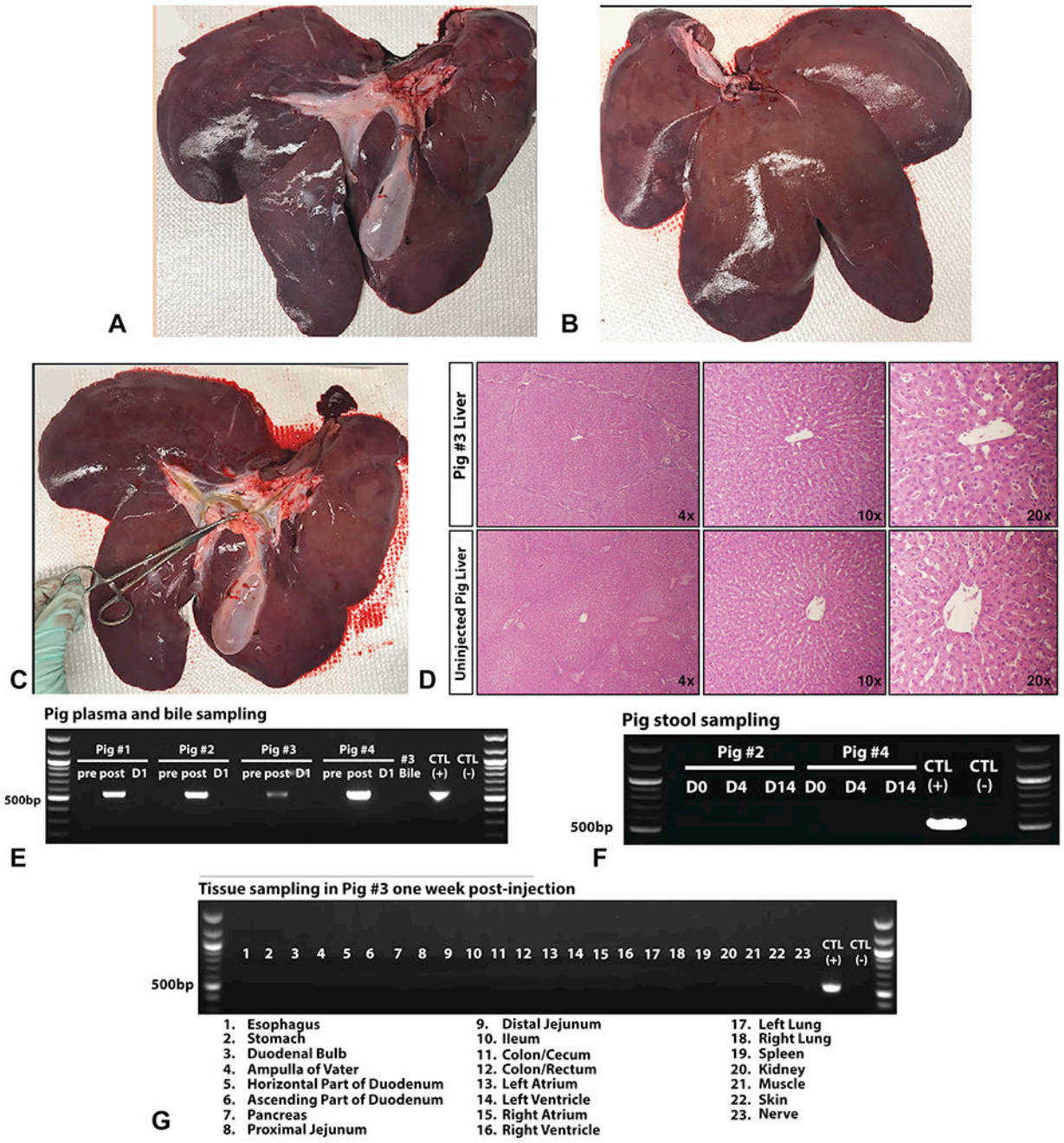

Figure 2. Pig liver is anatomically and histologically normal after hydrodynamic injection with no gene delivery into non-liver tissues.

A, The visceral liver surface of pig no. 3 one-week after injection is depicted with all 5 lobes observed along with the gall bladder and portal triad, showing no gross abnormalities. B, The diaphragmatic liver surface of pig no. 3 similarly shows no abnormalities. C, The intrahepatic biliary branches of pig no. 3 were dissected with no ruptures or lesions observed. D, Hydrodynamically injected pigs exhibited normal liver histology 1 week after injection. H&E stains are presented for pig no. 3 and a non-injected pig. PCR for hFIX DNA demonstrated the expected band size (550 bp). Positive control (CTL) is the hFIX plasmid,

and negative control is non-injected pig liver. E, pDNA biodistribution into porcine body fluids after hydrodynamic injection was studied. Plasma samples were taken preprocedure, 15 minutes postprocedure, and at day 1 (D) postprocedure for all 4 pigs. Bile tested by PCR at 1 week after injection during necropsy was negative. F, Stool samples were collected from pig no. 2 and no. 4 preprocedure, and at days 4 and 14 after injection were tested for hFIX DNA by PCR. G, Transfection of pDNA after hydrodynamic injection into non-liver tissues was not examined. A panel of 23 different tissues were sampled during necropsy in pig no. 3 one week after injection was tested by PCR.

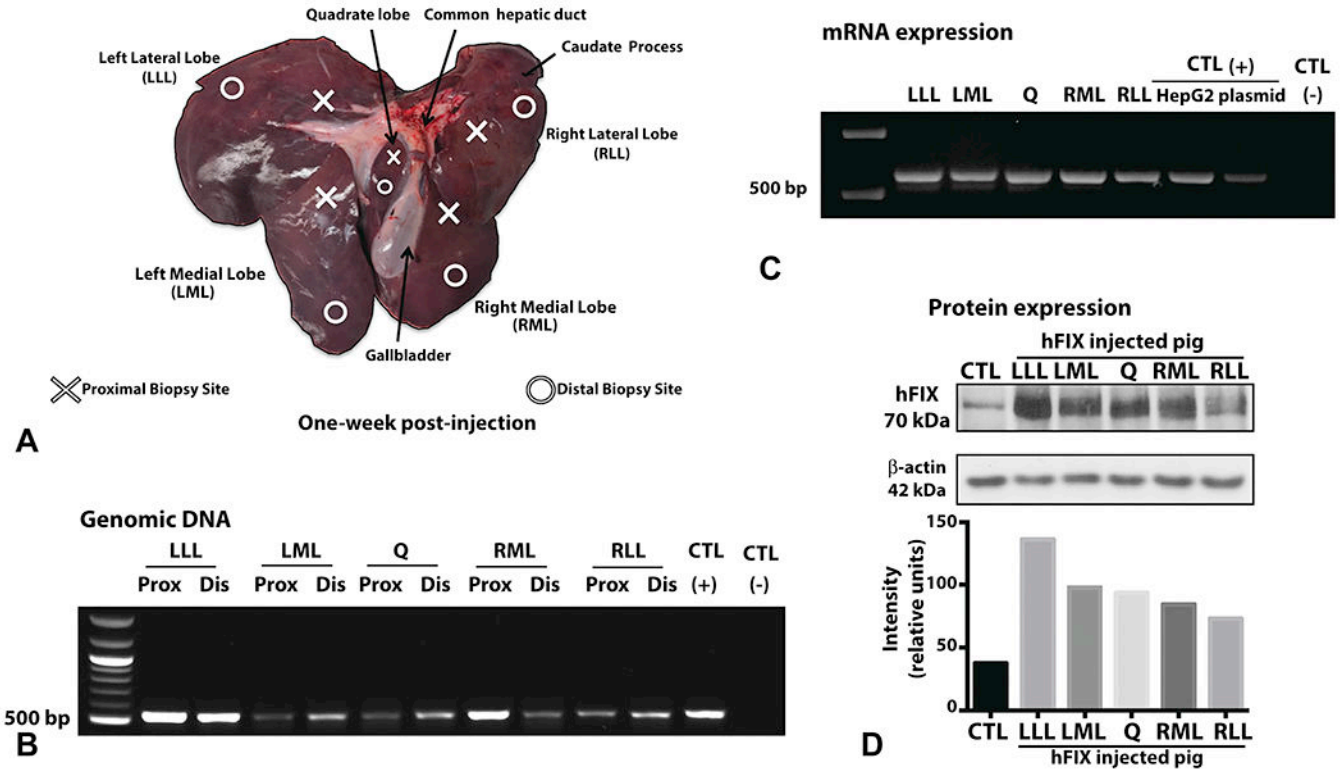

Figure 3. Biliary hydrodynamic injection mediates human FIX DNA delivery and protein expression in all liver lobes.

A, Tissue sampling scheme of pig liver across different lobes: right lateral lobe (RLL), right medial lobe (RML), left medial lobe (LML), left lateral lobe (LLL), and quadrate (Q) lobe. Proximal and distal samples to the site of catheter injection in the CHD were taken among all lobes. Pig no. 3 liver is depicted in A, harvested 1 week after injection for subsequent tissue analysis. B, PCR on genomic DNA revealed the expected band (550 bp) for hFIX DNA in all liver lobes tested. C, RT-PCR was performed on RNA extracted at 1 week after injection demonstrated the expected band size. RNA extracted from HepG2 cells transfected with pT-LP1-hFIX plasmid serves as one positive control. For both PCRs, positive control (CTL) is hFIX plasmid, and negative control is non-injected pig liver tissue. D, Western blot on liver tissue demonstrated the correct size of hFIX (70kDa) with a low-level cross reactivity for porcine FIX at the same molecular weight. Quantification of hFIX expression by western blot band intensity and normalized with beta-actin is provided. (CTL = control, non-injected pig liver).

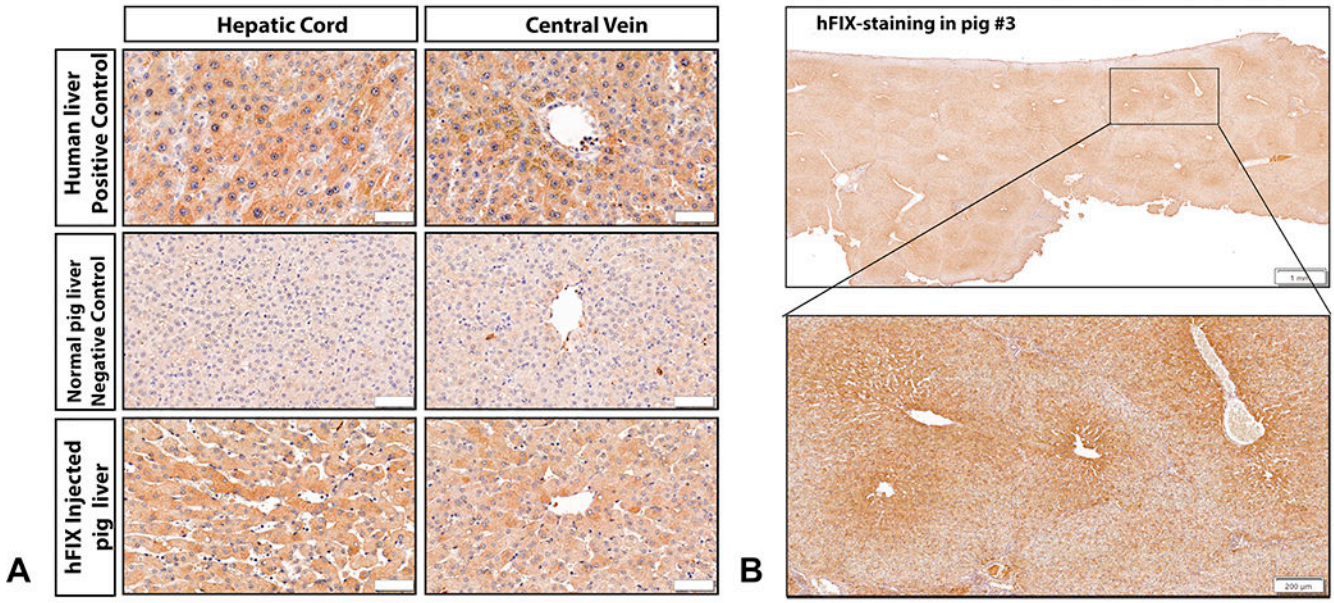

Figure 4. Immunohistochemistry shows efficient human Factor IX expression in pigs after hydrodynamic delivery.

A, IHC for hFIX in human liver tissue demonstrated homogenous, cytoplasmic expression in hepatocytes. Control tissue from a non-injected pig liver demonstrates only light background staining for porcine FIX appreciated. Immunostaining in hFIX-injected pig no. 3 revealed abundant hFIX-hepatocytes, with similar cytoplasmic staining to human hepatocytes with variable intensity (bar = 50 μm). B, An example of a liver section stained for hFIX at low magnification power is presented from pig no. 3, left medial lobe (LML) proximal section, demonstrating that immunostaining can be observed in every single lobule, with intensity highest in the center of the lobule (bar = 1 mm). A magnified image from the same liver biopsy section is also presented, showing intense staining bordering the central vein and radiating to the lobule borders (bar = 200 μm).

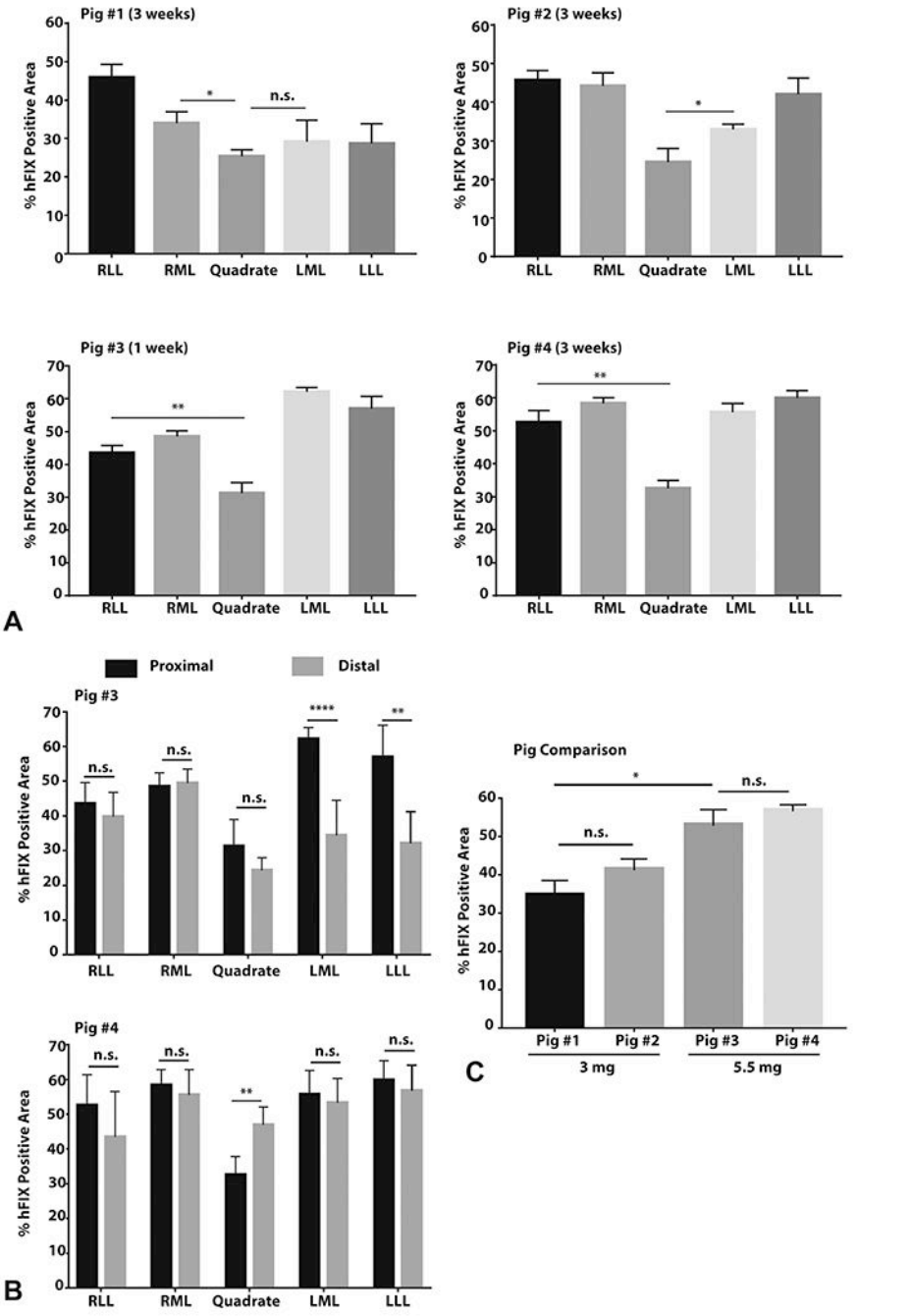

Figure 5. hFIX shows uniform distribution within the pig liver and successful expression in every pig after hydrodynamic injection.

The hFIX immunostained area within one hepatic lobule was quantified, and then 5 to 6 lobules were averaged to yield a liver lobe transfection value. A, The percentage area of hFIX-positive immunostaining within individual lobules (n=5-6) in pig no. 3 (1 week after injection) and pig no.1, no. 2, and no. 4 (3 weeks after injection) is provided. B, Among pig no. 3 and no. 4, distal and proximal portions of an individual hepatic lobe do not show consistent differences in percentage area of hFIX-positive hepatocytes (n=5-6). C, Higher doses of pDNA led to higher hFIX percentage area transfected. Each pig represents the

4 lobe averages determined in (A) now pooled together with quadrate lobe removed due to small size (~5% of the liver). Data measurements are presented as mean ± standard error of mean (SEM). Statistics represent unpaired, parametric, 2-tailed t-tests; significance ($p<0.05$). **** $p<0.0001$; ** $p<0.01$; * $p<0.05$; n.s. = not significant

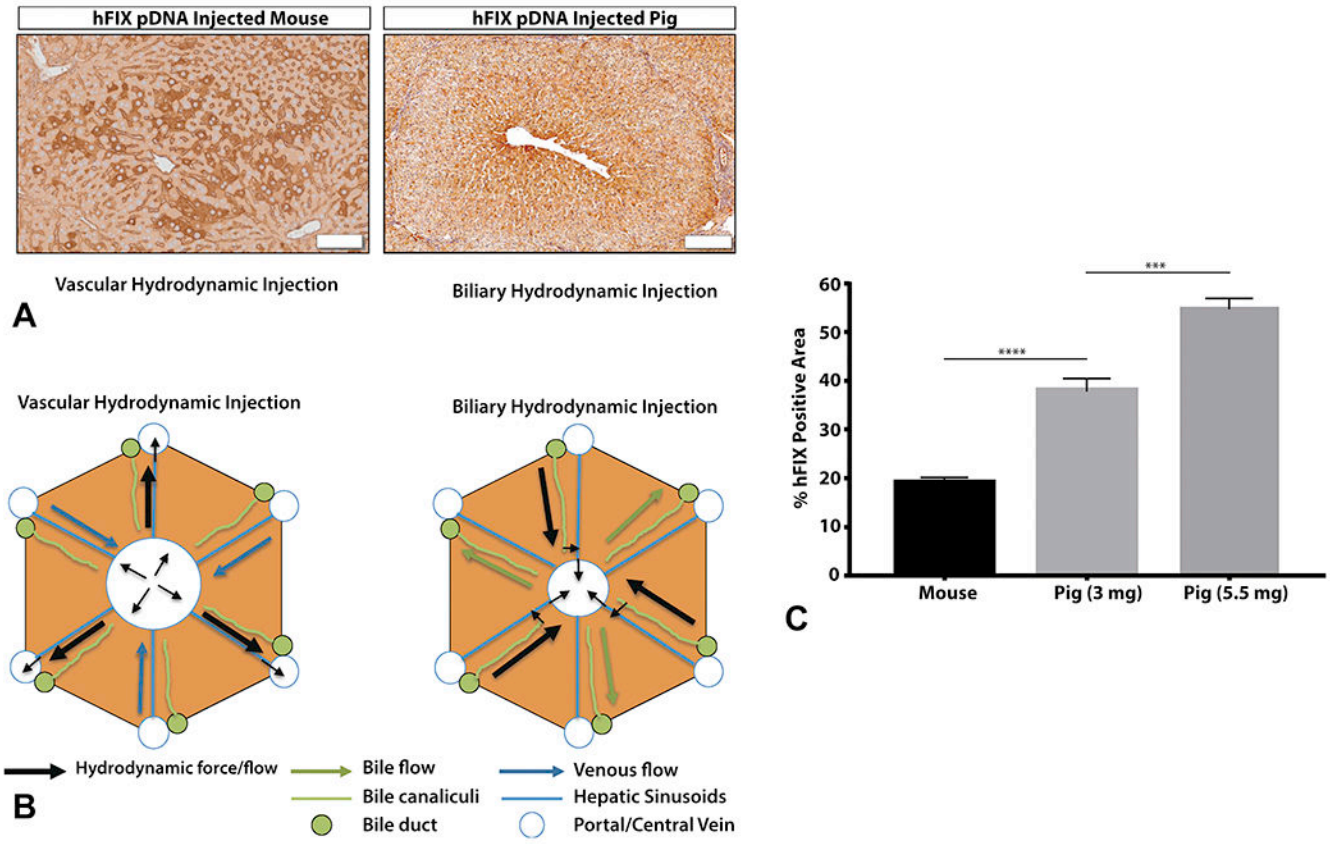

Figure 6. Pig biliary hydrodynamic injection yields superior transfection efficiency to mouse hydrodynamic tail vein injection.

A, Mouse HTVI is primarily located around central veins in zone 2 (bar = 50 μm). Pig hydrodynamic biliary injection leads to hFIX-positive expression almost uniformly circling central veins in zone 3 (bar = 200 μm), and then radiating outward along the chords reaching zone 1 and 2 (pig no. 3 LML proximal section depicted). Mouse lobules are smaller than pig lobules, respectively. B, A model of the mechanism of biliary versus vascular hydrodynamic delivery is presented, explaining the differences between pig and mouse hydrodynamic transfection results. C, For individual lobules, the percentage of hFIX-positive pig hepatocytes is significantly more than hFIX-positive mouse hepatocytes at matched DNA per liver weight doses (Mouse represents 3 mice, 18 lobules; Pig represents an average of 8 lobes from 2 pigs, with quadrate lobe excluded). Data measurements are presented as mean ± standard error of mean (SEM). Statistics represent unpaired, parametric, 2-tailed t-tests; significance ($p<0.05$). **** $p<0.0001$; ** $p<0.01$